Nanosecond repetitively pulsed discharges in N_2–O_2 mixtures: inception cloud and streamer emergence

2015 J. Phys. D: Appl. Phys. 48 175201

(http://iopscience.iop.org/0022-3727/48/17/175201)

IOP Publishing Journal of Physics D: Applied Physics
J. Phys. D: Appl. Phys. **48** (2015) 175201 (12pp) doi:10.1088/0022-3727/48/17/175201

Nanosecond repetitively pulsed discharges in N_2–O_2 mixtures: inception cloud and streamer emergence

She Chen[1], L C J Heijmans[2], Rong Zeng[1], S Nijdam[2] and U Ebert[2,3]

[1] Department of Electrical Engineering, Tsinghua University, 100084 Beijing, People's Republic of China
[2] Department of Applied Physics, Eindhoven University of Technology, PO Box 513, 5600 MB Eindhoven, The Netherlands
[3] Centrum Wiskunde & Informatica (CWI), PO Box 94079, 1090 GB Amsterdam, The Netherlands

E-mail: s.nijdam@tue.nl and chenshethu@gmail.com

Received 20 November 2014, revised 27 January 2015
Accepted for publication 9 March 2015
Published 27 March 2015

Abstract

We evaluate the nanosecond temporal evolution of tens of thousands of positive discharges in a 16 cm point-plane gap in high purity nitrogen 6.0 and in N_2–O_2 gas mixtures with oxygen contents of 100 ppm, 0.2%, 2% and 20%, for pressures between 66.7 and 200 mbar. The voltage pulses have amplitudes of 20 to 40 kV with rise times of 20 or 60 ns and repetition frequencies of 0.1 to 10 Hz. The discharges first rapidly form a growing cloud around the tip, then they expand much more slowly like a shell and finally after a stagnation stage they can break up into rapid streamers. The radius of cloud and shell in artificial air is about 10% below the theoretically predicted value and scales with pressure p as theoretically expected, while the observed scaling of time scales with p raises questions. We find characteristic dependences on the oxygen content. No cloud and shell stage can be seen in nitrogen 6.0, and streamers emerge immediately. The radius of cloud and shell increases with oxygen concentration. On the other hand, the stagnation time after the shell phase is maximal for the intermediate oxygen concentration of 0.1% and the number of streamers formed is minimal; here the cloud and shell phase seem to be particularly stable against destabilization into streamers.

Keywords: pulsed discharge, streamer, inception cloud

(Some figures may appear in colour only in the online journal)

1. Introduction

1.1. Streamer inception and its relevance

When the high voltage on an anode rises within (tens of) nanoseconds in air, discharge structures emerge that are very far from equilibrium and from the stationary state [1–4]. Streamer discharges are well-known as they also occur if the voltage rises more slowly, or even when dc voltage is applied. Nanosecond-resolved ICCD photography has shown that air streamers in pulsed discharges start from so-called inception clouds [5, 6] that initially form around strongly curved electrodes. When the voltage pulse lasts for only tens to hundreds of nanoseconds, the discharge may consist essentially of the inception cloud only. If the voltage pulse lasts longer, the inception cloud destabilizes and determines diameters and velocities of the emerging streamers. These stages of evolution are illustrated in figure 1.

So the inception cloud is the first stage of electric breakdown near a sharp electrode in a pulsed discharge in air, and the streamer channels emerge from it and extend further into regions with lower electric fields due to the electric field enhancement at their tips. In both, inception cloud and streamer, the electrons have energies in the eV regime while the gas remains mainly cold.

In industrial practice, transmission lines and electrodes in high voltage apparatus are elaborately designed to avoid streamer discharges, because streamers can lead to electrical energy loss, produce audible noise and radio interference or

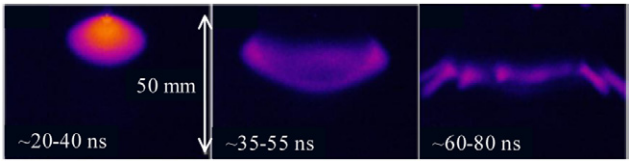

Figure 1. The initial stages of evolution of a pulsed positive discharge in air before the stage of streamer propagation: inception cloud (left), shell (middle) and destabilization of the shell into streamer channels (right). As will be shown later, a longer stagnation time can elapse until the cylindrical symmetry of cloud and shell are broken and streamer channels emerge. The time intervals of image exposure are indicated in the panels. Light is emitted from regions where additional ionization is created by electron impact during the opening time of the camera gate. A voltage pulse of 35 kV and of 130 ns duration is applied through the upper needle electrode to artificial air at 200 mbar. The electrode is the same as in the present investigation.

initiate dangerous short-circuits [8–10]. On the other hand, many chemically active species can be more energy-efficiently generated by streamers than by hot discharges like sparks. So streamer discharges are widely used in gas and water cleaning, ozone generation, and so on [11–13]. For the same reason, nanosecond pulsed discharges are very effective in generating chemical radicals for the ignition of combustible mixtures [14, 15]. Many researchers have investigated the macroscopic and microscopic mechanisms of streamer inception in order to either suppress or facilitate it. We will here make a step forward by analysing tens of thousands of discharges quantitatively under varying controlled conditions.

1.2. Discharge development

When a high voltage is suddenly applied to a sharp electrode in a nitrogen-oxygen mixture like air, the local electric field can increase to values above the breakdown field, i.e. to a field value in which electrons multiply as the impact ionization reaction creates more electrons than are lost due to attachment to oxygen If there are free electrons available, e.g. due to cosmic radiation, radioactivity or previous discharge activity, they will increase in number,. Negative oxygen ions can also be a source of free electrons, where O_2^- dominates at atmospheric pressure, and the detachment field for electrons from O_2^- is similar to the breakdown field. This is how plasma builds up in regions above the breakdown field [16–18] which will be denoted as E_c below.

As plasma builds up, charges separate and space charge effects set in. This happens in the inception cloud as well as in a streamer. In particular, the space charge layer around a long streamer channel will greatly enhance the electric field in front of its tip and suppress it in the conducting interior. If the enhanced electric field at the streamer tip stays above the breakdown value, the streamer will continue to propagate. But for a positive streamer to propagate with velocities comparable to electron drift against the electron drift direction, some electrons must be available in front of the streamer head. Their sources can be pre-ionization caused by natural ionization sources or by a laser [19], by leftover ionization of previous discharges, or by photoionizing radiation from the active ionization region of the streamer head [20–22].

Inception and development of streamers have been studied by many researchers. They mainly focus on the inception voltage or the electric field of streamers under nanosecond pulsed voltage, on lightning or switching impulse voltage or dc voltage [23–28]. And empirical or theoretical inception criteria are derived under different conditions. However, the detailed discharge evolution is still little investigated and understood. An important stage of development before the streamer emergence is the growth and break-up of the quasi-spherical inception cloud that forms around a sharp electrode [5, 21, 22].

1.3. Previous studies on inception clouds and streamer formation in pulsed discharges

1.3.1. Inception cloud. The term inception cloud was introduced by Briels *et al* [5] when they studied positive streamer inception in air at 100 and 400 mbar with nanosecond resolved photography with a voltage rise time of 25 ns. They found that the inception cloud developed into a growing shell and eventually broke up into streamers as illustrated in figure 1; here it should be noted that cloud, shell and streamers are the bright parts of the discharge where impact ionization is active at this stage of evolution; electric current can also flow in the dark parts. We remark that on uncommented pictures an inception cloud cannot easily be distinguished from a glow discharge at the electrode tip, but the glow is stationary while the inception cloud is strongly transient [3, 6].

Tardiveau *et al* [29] investigated nanosecond pulsed discharges in air with a 1.6 cm point-plane gap. The rise time of the voltage was 2–3 ns and the amplitude was +43 kV. When the pressure ranged between 1 bar and 3 bar, the discharge developed from what they call a diffuse pattern to a streamer mode. The so-called diffuse mode bears large similarities with the inception cloud observed earlier by Briels *et al* [5, 6], and the authors discuss a shell-like structure as well. For even higher pressures, the constriction and the branching of the discharge get stronger. Pechereau *et al* [30] recently observed essentially the same structure as Briels in figure 6 of [6], when they applied a voltage of 16–30 kV with a rise time of 2 ns to a 1 cm point-plane gap in atmospheric air. They observed an initially spherical ionization structure that due to the proximity of the opposite plate electrode developed into a conical discharge, while they did not relate their observation to the inception cloud concept that includes space charge effects. They also present 2D cylindrically symmetric simulations that reproduce the structure.

We remark that negative pulsed discharges in air form very prominent inception clouds as well that might not break up into streamers at all [31], this is related to the fact that lateral electron drift suppresses field enhancement in negative streamers and makes them more difficult to form [32].

The influence of small changes in voltage rise time on the positive inception cloud has been investigated by Clevis *et al* in pure nitrogen [33]. They found that discharges with a shorter voltage rise time form a larger inception cloud and

have a lower average velocity. They relate the lower average velocity to the larger inception cloud that grows more slowly than the streamers and also stagnates before breaking up into streamers. Therefore a longer inception cloud stage with a larger cloud will cause a lower average velocity.

In general, inception clouds form before many pulsed positive streamer discharges, but they are most prominent in air. In gases like pure nitrogen and pure argon the inception cloud seems to break up quickly if it forms at all; this is probably related to the gas dependence of breakdown dynamics above the breakdown field [16–18]. In fact, in the present paper we will find that in high purity nitrogen no inception cloud is formed at all.

The theoretical maximum size of the cloud and shell is estimated in [21, 33]. The inception cloud is approximated as spherical and ideally conducting. The electric field E on the surface of a perfectly conducting sphere is U/R for radius R and applied voltage U. The cloud can continue to grow until the electric field on its surface equals the breakdown field E_c of the gas. Therefore the maximal radius $R_{\max}$ of the shell can be estimated as $R_{\max} = U/E_c$. The measured shell size in artificial air is somewhat smaller than the theoretical radius, as we will also quantify later in this paper. The deviation of measurements from this theoretical approximation can be due to the non-spherical shape of the cloud, to its finite conductivity, and to the fact that the electron density created behind the ionization front depends on the electric field and vanishes when the breakdown field is reached; therefore the latest growth stage might not be visible.

1.3.2. Streamers in different nitrogen–oxygen mixtures. Nijdam *et al* [21] studied the influence of the oxygen ratio in nitrogen–oxygen mixtures on the morphology of fully developed streamer channels. They investigated pure nitrogen and nitrogen with 20%, 0.2% and 0.01% oxygen and found that the inception cloud was hardly visible in pure nitrogen. Remarkably, the experimental results showed that the average streamer velocity is similar for all nitrogen–oxygen mixtures, despite their very different morphology. Furthermore, the influence of background ionization was investigated in [22] by varying the voltage pulse repetition frequency and by using a radioactive admixture. In the experiments, a Blumlein pulser was used to create a rectangular voltage pulse with a rise time of about 10 ns and length of about 130 ns. With the repetition rates increasing from 0.01 Hz to 10 Hz, the inception clouds become smaller. Simultaneously, the streamers become longer and thicker.

1.3.3. Similarity laws between discharges at different pressures. Another important aspect in streamer investigations are the scaling laws relating discharges at different gas densities [6, 34–38]. Thin streamers in laboratory experiments at pressures of 10 to 1000 mbar and large scale sprites at pressures as low as 10 μbar high up in the atmosphere show many physical similarities. The mean free path λ of the electrons determines the length scales in the streamer tip; it is inversely proportional to the molecular density n, $\lambda \sim 1/n$. Over this length the electron gains the energy $e\mathbf{E}\lambda$ in a local electric field $\mathbf{E}$. The energy should be compared to the ionization threshold of the gas molecules on which the electron impacts and is thus independent of n. Therefore at different densities n with the same reduced electric field $|\mathbf{E}|/n$, the discharges are physically similar when lengths, times, velocities and densities are rescaled with appropriate factors. However, the validity of the scaling laws is limited to the fast two-body processes in the impact ionization front at the streamer tip, where charged particles collide with the neutral molecules of the background gas. On the other hand, electron loss and electron storage in negative ions proceed either through two-body or through three body processes, forming O^- or O_2^-, depending on air density [18, 39–41]. For a discussion of further corrections due to the presence of electrodes, to the discrete particle fluctuations and so on, we refer to [35].

1.4. Contents of the paper

In this paper, we present experiments on the detailed temporal evolution of inception clouds and their break-up into streamers in gases with varying nitrogen–oxygen ratio, pressure and under different voltage amplitudes and rise times. In contrast to earlier studies, we present extensive statistics over tens of thousands of discharges which allow us to pinpoint generic behaviour and the range of fluctuations. Section 2 discusses experimental set-up and methods, section 3 the main experimental results, and section 4 a discussion of evolution stages and physical mechanisms.

2. Experimental setup and methods

The discharges are generated in a point-plane electrode configuration with a gap distance of 16 cm. The electrodes are placed in a vacuum vessel that maintains the high purity of the investigated gases. The set-up was described in detail in [21]. In our experiments, nitrogen 6.0 (i.e. with less than 1 ppm total impurities) and N_2–O_2 gas mixtures with oxygen contents of 100 ppm, 0.2%, 2% and 20% were investigated, mostly at 100 mbar and always at room temperature. A gas flow of 400 sccm was pumped into the vessel during the measurements in order to replace the gas every 25 min at 100 mbar.

The voltage pulses were produced by the so-called C-supply circuit that was treated extensively in [42]. In this circuit a capacitor is charged by an external dc voltage supply through a charge resistance. After the spark gap, which is connected to one side of the capacitor, is triggered by a thyristor switch, a positive voltage at the other end of the capacitor is applied to the electrode tip. The generated voltage pulses have amplitudes of +20, 26 or 30 kV, rise times of 20 or 60 ns and durations at half maximum of 10 μs; they are applied with repetition frequencies of 0.1, 1 or 10 Hz. A sketch of the voltage pulses is included in figure 2. The current through the plane electrode is measured by a 50 Ω shunt impedance. The bandwidth of the current measurement system has been determined to be at least 35 MHz.

The positive discharges are imaged by an ICCD camera with variable times for opening and closing the image

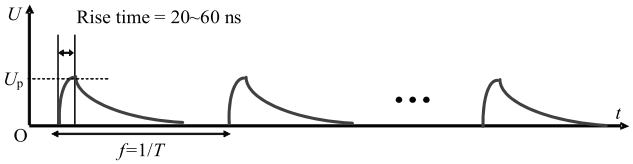

Figure 2. A sketch of voltage pulses with amplitude U_p and repetition frequency f.

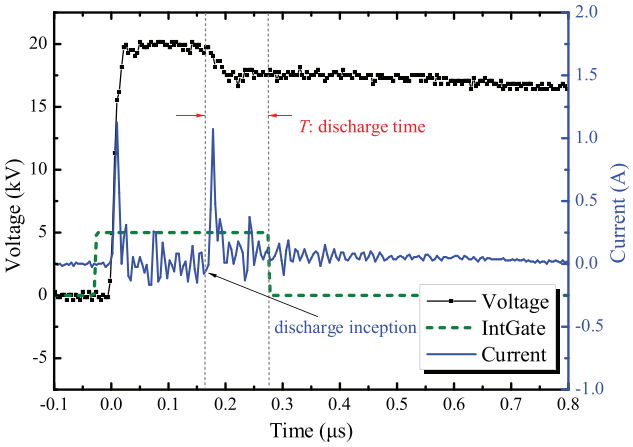

Figure 3. The waveforms of voltage, current, and camera internal gate signal. IntGate is the gate signal of the ICCD camera where a high voltage indicates that the gate is open. T is the time between the start of the discharge current and the end of the camera exposure; we will use the term 'discharge time' for this time span below.

intensifier of the camera, and voltage, current and the camera internal gate signal are recorded. In almost all measurements presented here, the camera gate opens before the discharge starts. As there can be a jitter of tens of nanoseconds between the voltage rise and the discharge inception, we define the discharge time for an image as the time between the measured rise of the second current pulse and the camera gate closure. The first current pulse is the capacitive current due to the voltage rise and the second one is the current due to the discharge inception. This is illustrated in figure 3 where a typical voltage and current waveform are shown together with the camera timing. In this way, one obtains an accurate relationship between the longest discharge propagation distance and the elapsed time since inception. We remark that the large time delay between the voltage rise and the discharge inception in figure 3 is exceptional and that the average delay is tens of nanoseconds.

The synchronizing procedure is performed as the following steps. First the initial trigger of each streamer discharge is created by a function generator. The signal from the function generator is converted to an optical signal and then sent through an optical fiber into the high voltage setup. Then the spark gap can be triggered to apply voltage to the tip. In the meantime, the initial signal is used to fire the ICCD camera and to trigger the oscilloscope to record the voltage and current waveform. Only one picture per discharge can be taken due to the long read-out time of the camera, of the order of 1 fps. Important is the opening and the closing time of the camera

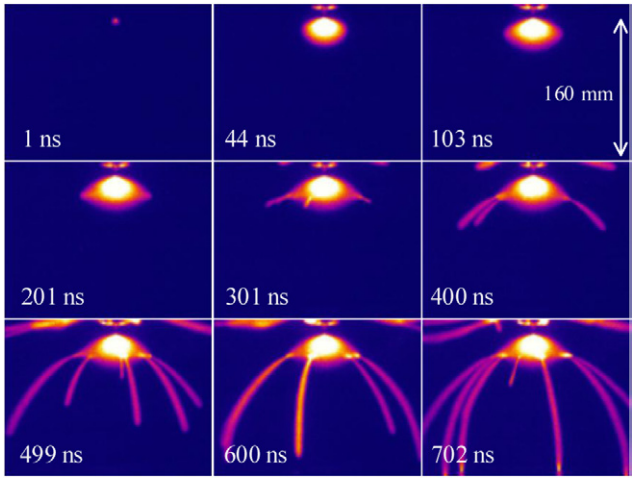

Figure 4. Time integrated images of discharges in 100 mbar artificial air with a voltage amplitude of +20 kV and a rise time of 20 ns at a repetition frequency of 1 Hz. The discharge time from the start of the discharge current to the end of exposure is indicated in each image. Each image is from a different discharge pulse under the same conditions.

relative to voltage and current signal that can be adjusted with nanosecond precision. A detailed analysis of the timings and delays has been performed in [43].

Over 10 000 ICCD discharge images with varying camera gate closure time were taken to obtain the results presented here. All images presented in the figures have been optimized by changing contrast to get a better visual quality. The approach is similar to [2, 5, 33, 44]. But the number of evaluated images is much larger. In each image the longest discharge propagation distance as measured from the tip was automatically selected, and its length was calculated in Matlab. The longest lengths of these discharges are then plotted as function of the discharge time, giving very accurate information on average discharge development and jitter.

3. Experimental results

3.1. General development of the discharge

Figure 4 shows representative discharge images in 100 mbar artificial air (80% N_2 and 20% O_2) at a voltage amplitude of +20 kV, a voltage rise time of 20 ns and a pulse repetition frequency of 1 Hz. These parameters will be our standard setting in this paper, and later we will vary individual parameters separately. After 44 ns a large inception cloud has formed that slowly increases further. It destabilizes and forms streamers after about 300 ns. These streamers reach the planar electrode after 600–700 ns.

Similar developments were observed previously in [3, 5–7, 33]. While the photographs in figure 4 show the integrated light emission intensity since the start of the discharge, those earlier publications show in time resolved images (see figure 1) that light is emitted first from a growing cloud around the tip, and later from a shell around the previous cloud, i.e. ionization first occurs in a compact volume and later in an ionization front at the edge of the cloud, indicating that the electric field

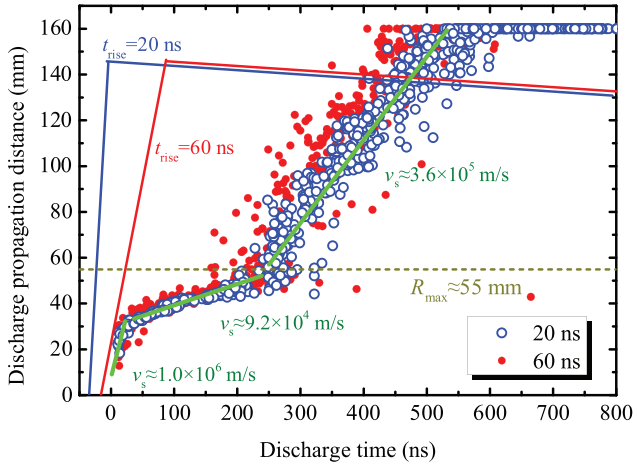

Figure 5. Discharge development plot: the largest extension of the discharge from the needle tip is plotted as a function of discharge time. The discharges are created only in 100 mbar artificial air with a voltage amplitude of 20 kV at a repetition frequency of 1 Hz. The rise time of the pulse voltage is 20 ns or 60 ns as indicated and drawn schematically with solid blue and red lines. The green lines are linear fits of the data at various stages with corresponding propagation velocities indicated. The R_{max} line (olive dashes) is drawn where the velocity changes clearly; this is our evaluation of the maximal shell radius R_{max} from the experiments.

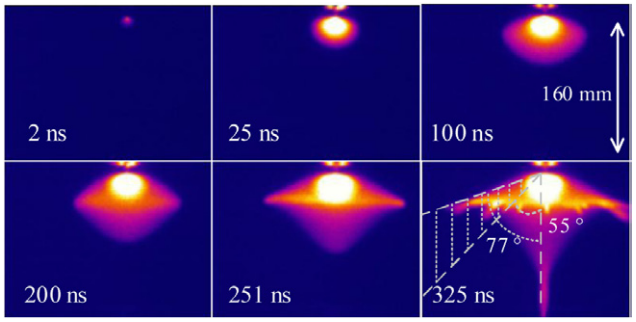

Figure 6. Time integrated images of the discharge in 100 mbar artificial air with a voltage amplitude of +30 kV at a repetition frequency of 1 Hz. The area indicated with dashed and dotted lines in the lower right picture is where the lateral discharge propagation distance of figure 7(*b*) was evaluated.

in the cloud is now largely screened. The shell then eventually breaks up into streamers whose largely varying diameters and velocities [42, 45] are determined by the properties of inception cloud and shell. In the time integrated images of figure 3, this development can be deduced from the changes from one image to the next. In particular, the cloud stagnates and hardly emits light between 100 and 300 ns which is reflected by the fact that the time integrated images don't change when the discharge time increases.

We remark that figure 4 also shows a few streamers emerging from the upper part of the electrode tip. We assume that these streamers do not influence the development and break-up of the inception cloud.

We now use 700 images on average with different gate times to quantify the discharge development as a function of the discharge time. Note that each image is from a different discharge event as the ICCD camera has a limited frame rate. The jitter between different discharges under the same conditions can be read from the discharge development plot as shown in figure 5.

3.2. Effect of voltage pulse

3.2.1. Voltage rise time. Here we study the influence of the voltage rise time on the discharge development in artificial air. The voltage rise time of the C-supply can be varied by changing a resistor. The longest discharge propagation distance as a function of the discharge time T since the start of the discharge is plotted in figure 5 for rise times of 20 and 60 ns. (Distance and time were defined in section 2.)

Initially the inception cloud develops very rapidly with a velocity of about 1.0×10^6 m s^{-1}, and then the shell expands with a velocity decreasing to 9.2×10^4 m s^{-1}, up to a radius of about 55 mm from the tip. We define the maximal shell radius R_{max} in these measurements as the radius where the velocity changes clearly. Sometimes a stagnation can be seen after the shell phase. Then streamers emerge and propagate with a velocity of 3.6×10^5 m s^{-1} towards the planar electrode. The break-up of the inception cloud is a stochastic process and has a jitter of approximately 100 ns under the present conditions.

In the early stage the inception cloud expands a bit faster for the faster rise time of 20 ns. Moreover, these discharges appear to form a more stable inception cloud that breaks up later though the voltage at the time of break-up is the same. For the 20 ns rise time, the initial fast growth stage of the discharge (which is the inception cloud phase) takes place when the voltage has already reached its maximal value, while the voltage is still increasing in the case of the 60 ns rise time. Therefore, the electric field is higher for 20 ns rise time during the initial stages of cloud formation. It can create a higher electron density and conductivity in the inner part of the cloud, allowing the cloud surface to be closer to equipotential. With a 60 ns voltage rise time the inception cloud grows more slowly, but breaks up earlier. The average streamer velocity v_s is similar (3.6×10^5 m s^{-1}) for the two rise times. The velocity measured here is less than the average discharge velocity (8.0×10^5 m s^{-1}) in [33] since an even faster rise time of 10 ns was used there.

3.2.2. Voltage amplitude. Now we investigate the effect of the voltage amplitude while keeping all other parameters constant. The discharge development in artificial air with 30 kV voltage amplitude is illustrated in figure 6, for comparison with the plots at 20 kV in figure 4.

Again the inception cloud is first growing rapidly and then decelerates. Its maximal radius now reaches 85 mm. Then the cloud breaks up, and in most cases it forms a single streamer on the symmetry axis that then propagates towards the cathode plane. Meanwhile many small branches emerge at the lateral edge of the cloud. At 20 kV amplitude the streamers from the edge of the cloud reach the plane earlier in most cases. For the higher voltage amplitudes the inception cloud is so close to the cathode plane that the electric field is largely enhanced in this direction. Therefore the streamers initiate more easily in that region than from the lateral edge of the inception cloud.

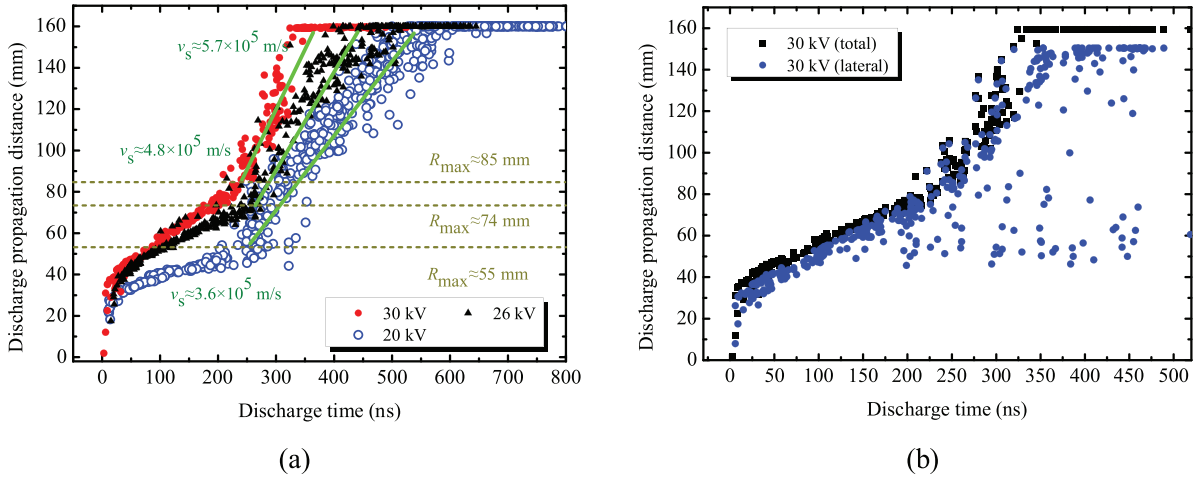

Figure 7. (*a*) Voltage dependence of the discharge development, for voltage amplitudes of 20 kV, 26 kV and 30 kV. Again only in 100 mbar artificial air at a repetition frequency of 1 Hz and voltage rise time of 20 ns. (*b*) Comparison of streamer lengths in the total area and only in the lateral area as indicated in figure 6.

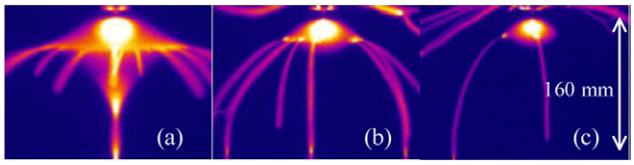

Figure 8. Discharge morphology at different pressures (artificial air, 20 kV, 1 Hz): (*a*) 66.7 mbar, (*b*) 100 mbar, (*c*) 125 mbar.

Figure 7(*a*) shows the influence of voltage amplitude in a discharge development plot. The size of the inception cloud increases with increasing voltage amplitude. It is 85 mm at 30 kV, which is approximately 1.5 times as large as at 20 kV. The average streamer propagation velocity shows the same trend, as the velocity at 30 kV is also 1.5 times as large as at 20 kV ($5.7 \times 10^5\,\mathrm{m\,s^{-1}}$ versus $3.6 \times 10^5\,\mathrm{m\,s^{-1}}$). Moreover, for higher voltages the stagnation of the inception cloud is much less pronounced and its break-up appears less stochastic in nature. The discharge propagation distance on the lateral side of the inception cloud is plotted in figure 7(*b*). The region of these lateral measurements is indicated with dashed and dotted lines in figure 6. After the inception cloud phase, the lateral streamers start a bit later, but during 20–200 ns, they appear to catch up with the central ones and thus to propagate faster. The clearest difference can be seen between 300 and 350 ns, where the central streamers make their final jump to the cathode. During this phase, the lateral streamers propagate more slowly than those in the center of the gap, and sometimes they stop propagating altogether.

3.3. Effect of pressure and pulse frequency

Before changing the nitrogen oxygen ratio in section 3.4, we will change the gas composition slightly in two other ways. First, we will change pressure. As discussed in the introduction, an ionization front should propagate in essentially the same manner, but photo-ionization is a bit enhanced at lower pressures [46]. However, the relative importance of two-body versus three-body processes in, e.g. electron loss and gain rates ahead of the streamer and in the streamer channel differs. In this context we will also investigate whether the discharges scale with pressure. Second, we will change the pulse repetition frequency which influences density and distribution of the ion density remaining from the previous discharge. (We remark that the electron density remaining from the previous discharge should be negligible at these repetition frequencies in air [19].)

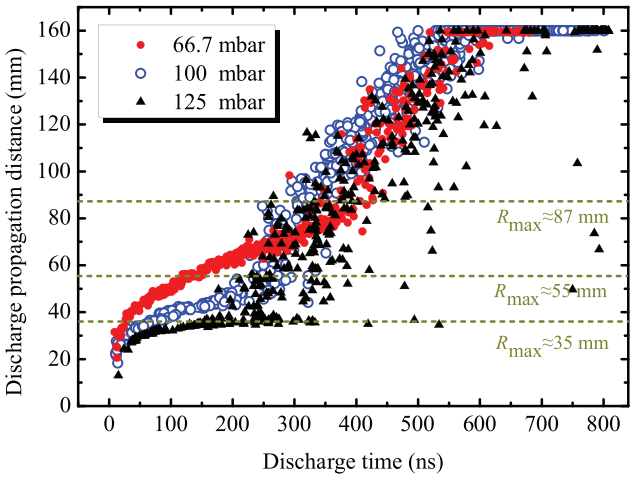

Figure 9. Pressure dependence of the discharge development, for pressures of 66.7, 100, and 125 mbar. Again in artificial air with voltage amplitude of 20 kV and rise time of 20 ns at a repetition frequency of 1 Hz.

3.3.1. Pressure. Here the voltage is kept fixed at 20 kV and the pressure is increased. Figure 8 shows the morphology of the streamers for pressures of 66.7, 100 and 125 mbar. At higher pressure the inception cloud is smaller, and the number of streamers breaking out of the inception cloud is smaller.

The discharge development is plotted in figure 9. The measured sizes of the clouds and shells are about 87, 55, and 35 mm for the three pressures. The time of the break-up decreases with increasing pressure, but the jitter of this time increases. The velocity of the streamers is roughly the same.

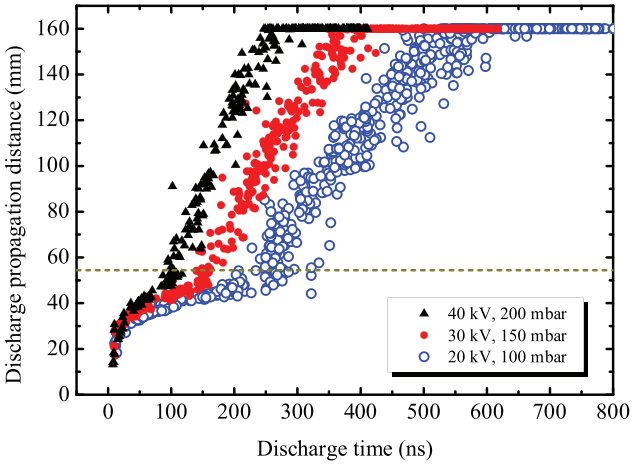

Figure 10. Scaling of the discharge development, for three combinations of voltage amplitude U_p and pressure p with U_p/p kept constant. Again in artificial air at a repetition frequency of 1 Hz and voltage rise time of 20 ns.

3.3.2. Investigation of scaling with pressure. Streamer diameters generally scale well with gas density n [6, 38] when field and gas density are changed while the reduced electric field $|\boldsymbol{E}|/n$ is kept constant. We will investigate now the scaling of the whole discharge development. The measured pressure p is proportional to n according to the ideal gas law as our experiments were all performed at room temperature. The background electric field strength is proportional to the voltage amplitude U. Therefore we use the ratio U/p as substitute for the reduced electric field $|\boldsymbol{E}|/n$ in our laboratory experiments, and investigate the discharge development by changing the maximal voltage amplitude U_p and the pressure p by the same factor. The results are plotted in figure 10. The size of the cloud and shell is nearly the same for the three different U_p and p combinations with the same value of U_p/p. But for higher U_p and p the whole evolution is faster: the clouds form and break up more rapidly, and the streamers are faster. We will give a physical interpretation of this nontrivial fact in section 4. Furthermore, the jitter of the break-up time is less, not only in absolute numbers, but even relative to the break-up time.

3.3.3. Repetition frequency. Since the discharges produce high ionization levels, they can increase the level of background ionization for subsequent discharges [20, 22]. In gas mixtures with high oxygen concentrations, ionization is mostly present in the form of negative and positive ions near STP conditions on a time scale of seconds. Clearly these background ionization levels change with repetition rate [22].

The discharge development at 0.1, 1, and 10 Hz repetition frequency is plotted in figure 11(*a*) for otherwise the same parameters as before. For 10 Hz and 1 Hz repetition frequencies the cloud and shell grows up to a maximal radius of about 55 mm while for 0.1 Hz its maximal size is about 45 mm. Furthermore, at this repetition frequency some discharges do not grow any further as no streamers emerge from the inception cloud. This is shown in figure 11(*b*) where the number of streamers breaking out of the inception cloud is plotted as a histogram. For 0.1 Hz repetition frequency, there are only two streamers on average while for 1 and 10 Hz, there are about 6. One can conclude that at the higher frequencies inhomogeneously distributed background ionization from the previous discharge plays a role in destabilizing the inception cloud.

3.4. Effect of N_2–O_2 ratio

In order to investigate the influence of oxygen concentration, we use nitrogen–oxygen mixtures with oxygen concentrations of 20% (artificial air), 2%, 0.2%, 100 ppm (N_2 4.0) and 1 ppm (N_2 6.0). Figure 12 shows the typical photographs with a long gate time of about 1000 ns. Similar figures were shown in [21] for different voltage and pressure.

For 2% and 0.2% O_2 the size of inception cloud and shell is almost as large as for artificial air. It decreases to 31 mm in N_2 4.0 while hardly any inception cloud can be distinguished in N_2 6.0. This last observation is investigated in more detail in figure 13 by zooming in to the region around the tip that is indicated by the dashed white rectangle in figure 12(*a*), and by using a shorter exposure time. Two bright spots can be seen on the tip in the first image during the time interval of 3–5 ns, which might imply that there are already separate streamers initiating from the tip instead of a smoothly expanding cloud. On the other hand, in the next two images during 9–17 ns, there is a cloud like structure. There is some randomness in these early images and sometimes the edge of the cloud is irregular and sometimes smooth. However, no shell-like ionization fronts emerge as described by Briels *et al* [5] in air, and illustrated in figure 1; this seems to indicate that space charge effects do not play an important role in N_2 6.0 before the streamer stage. Rather many streamers appear directly from the small cloud within a few nanoseconds. This phenomenon is different from Clevis's findings [33]. There the inception cloud in nitrogen 6.0 was likely to form and grow to a larger size. However, they used a higher voltage of 25 kV, a shorter rise time of 10 ns and a higher repetition rate of 5 Hz instead of our 1 Hz. The research results shows that the inception voltage is higher for faster rise times [23]. The faster rise time and higher voltage amplitudes in Clevis's experiments will create a higher electric field around the tip. In that large overvolted region. More electron avalanches may be produced and thus the inception cloud is more likely to form.

Furthermore, figure 12 shows that many streamers emerge from the cloud in 0.01% O_2. But in 0.2% O_2 and 2% O_2 usually less than 3 streamers break up from the inception cloud while in artificial air the streamer number increases. We will now quantify these observations.

Figure 14 shows how the discharges develop in different N_2–O_2 mixtures. In the high purity nitrogen (N_2 6.0), the discharges propagate at an average velocity of $5.7 \times 10^5\,\mathrm{m\,s^{-1}}$ throughout the gap. While the earlier plots in air all showed stagnation between the development of the inception cloud and the formation and propagation of streamers, here no stagnation is visible: after an initial fast growth the discharges decelerate to a constant velocity in the streamer phase. This is consistent with the observation that deceleration and stagnation appear during and after the shell phase in air, and that there is no shell phase visible in the high purity nitrogen.

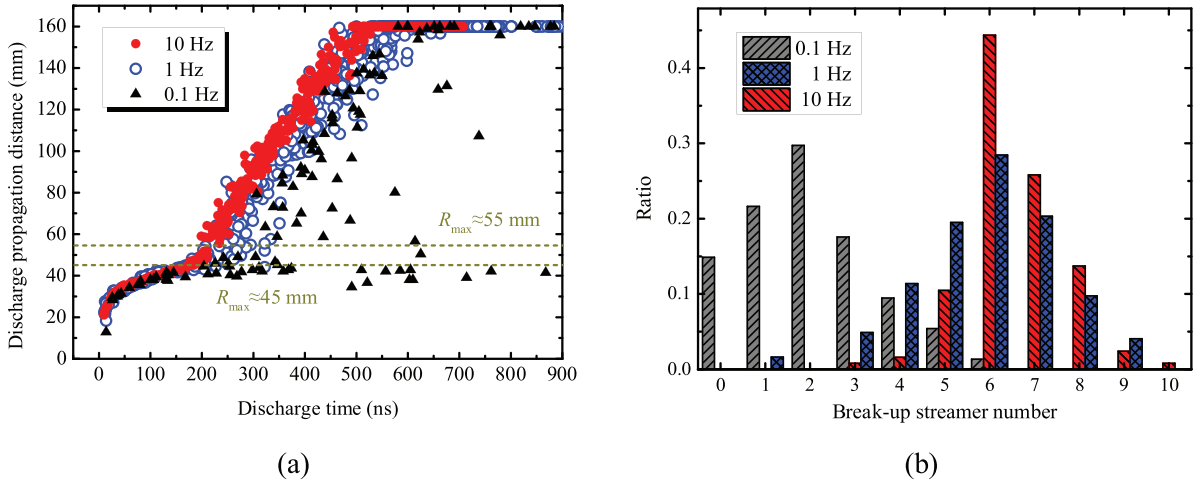

Figure 11. (*a*) Frequency dependence of discharge development, for pulse repetition frequencies of 10 Hz, 1 Hz, and 0.1 Hz. Again in 100 mbar artificial air with voltage amplitude of 20 kV and rise time of 20 ns. (*b*) A histogram of the number of break-up streamers at the three repetition frequencies.

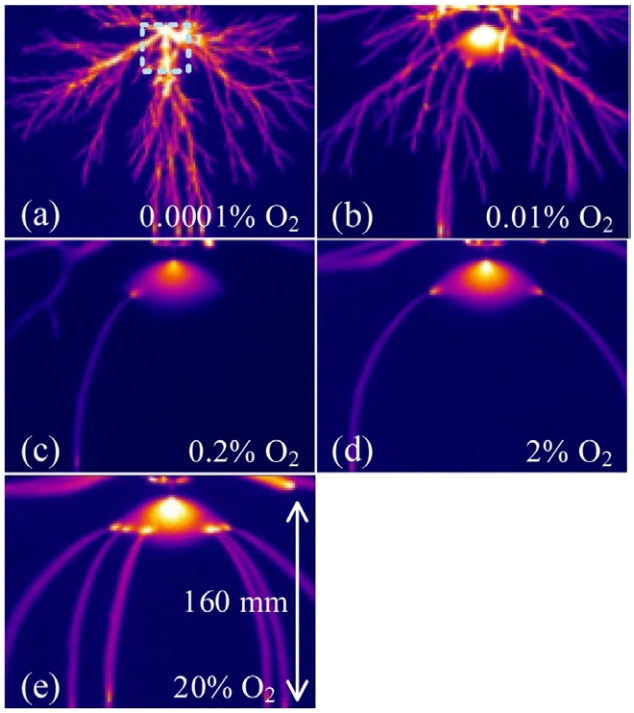

Figure 12. Discharge morphology in different gas mixtures (100 mbar, 20 kV, 1 Hz): (*a*) N_2 6.0 (<0.0001% O_2), (*b*) N_2 4.0 (0.01% O_2), (*c*) 0.2% O_2 + 99.8% N_2, (*d*) 2% O_2 + 98% N_2, (*e*) artificial air (20% O_2 + 80% N_2).

When the streamers have almost reached the cathode plate they make a short jump across the final gap, due to the proximity of the electrode that enhances the electric field ahead of the tip further and provides electrons by secondary emission.

In N_2 4.0 a small delay between the growth of the inception cloud and its break-up can be seen, but it is mostly hidden in jitter. In gas mixtures with higher oxygen concentrations, the inception cloud develops at a similar velocity at first, then their velocity decreases largely during the shell phase. After this stagnation phase the cloud breaks up into separate streamers that propagate with a typical velocity around $3.6 \times 10^5\,\mathrm{m\,s^{-1}}$. In the mixtures with the intermediate oxygen concentrations of 2% and 0.2%, the stagnation time becomes as long as 300–700 ns; moreover the jitter is of similar size and in a large number of cases the inception cloud does not break up at all until the end of the measurement. The stagnation time decreases to about 240 ns for the highest oxygen concentration of 20%, the jitter to 80 ns, and the inception cloud always breaks up.

The growth velocities of the inception clouds in the first tens of nanoseconds before stagnation are quite similar for all gas mixtures, and they are always larger than the streamer velocities.

The streamer stagnation time as a function of oxygen concentration is plotted in figure 15(*a*). It is shortest in pure nitrogen and has a maximum of 520 ns at 0.1% oxygen. The jitter of streamer break-up time is also the largest at 0.1% oxygen approximately. Figure 15(*b*) shows a histogram of the number of break-up streamers as a function of oxygen concentration for concentration of 0.2%, 2% and 20%. N_2 6.0 and N_2 4.0 are not included because there are so many break-up streamers that they overlap and cannot be counted easily. While the streamer stagnation time is maximal for the intermediate oxygen concentration of 0.1% or 0.2 %, the number of streamers formed after break-up is minimal, 1 on average. This indicates that inception cloud and shell are particularly stable at these intermediate oxygen concentrations.

4. Discussion and interpretation

The discharge develops in general in a sequence of inception cloud, shell formation, discharge stagnation and break-up into streamers, except in the high purity nitrogen where streamers seem to form rather immediately.

4.1. The inception cloud

4.1.1. The size of the cloud and shell. As discussed in the introduction, an easy estimate shows that the ionization cloud

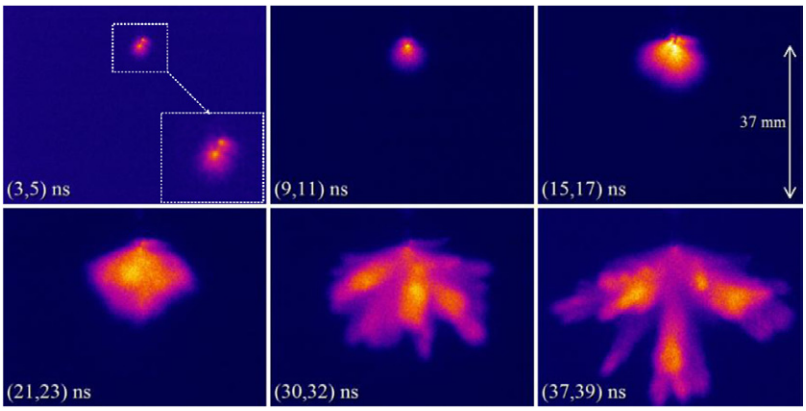

Figure 13. Time resolved images of the early discharge development in pure nitrogen with zoom-in view (100 mbar, +20 kV, 1 Hz). The exposure time of each image is 2 ns and the times in brackets indicate start and end of the gate time with reference to the discharge inception.

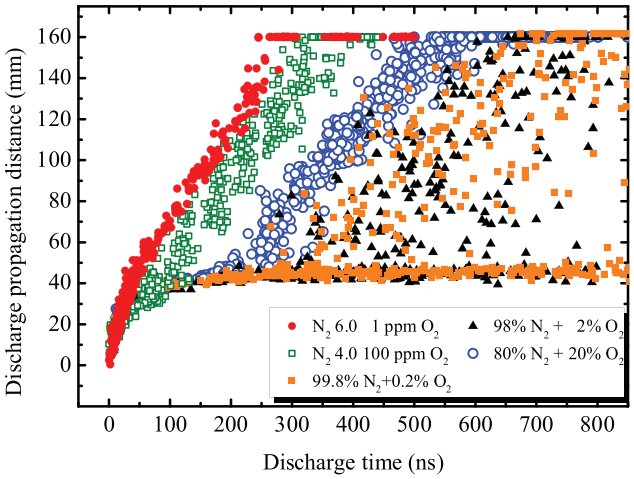

Figure 14. Discharge development for different gas mixtures. Again in 100 mbar gases with voltage amplitude of 20 kV and rise time of 20 ns at a repetition frequency of 1 Hz.

in air cannot become larger than U_p/E_c where E_c is the breakdown field. This field can be approximated as $E_c = 32\,\mathrm{kV\,cm^{-1}} \cdot p/1\,\mathrm{bar}$ in air at room temperature where p is pressure. We consider the tip as the center of cloud or shell, and then we measure the maximal radius in different directions. Table 1 shows the measured and predicted sizes of the clouds in air for varying voltage amplitude U_p and pressure p.

First, the data confirm that the size of the cloud and shell obeys the similarity laws with pressure: the size depends only on U_p/p. Second, the theoretical estimate is typically 8–14 % larger than the measured value, with the exception of the case (20 kV, 125 mbar) where the measured value is 30 % smaller.

That U_p/E_c is larger than the measured size, can be related to the fact, that (1) the estimate assumed that the full voltage U on the electrode is also on the outer boundary of the cloud, while there might be a potential drop within the cloud so that the real voltage on the boundary is smaller, and that (2) in the final growth phase the electric field at the outer boundary of the cloud is very close to the breakdown field; in this case very little ionization is created in the ionization front, and the faint luminescence might not be captured by the camera. Furthermore, the cloud is, of course, not perfectly spherical as the electrode needle enters from one side.

Table 1. Measured sizes of the inception cloud and shell and theoretical upper bound U_p/E_c in air for varying voltage amplitude U_p and pressure p.

U_p [kV]	P [mbar]	Measured size [mm]	U_p/E_c [mm]
20	100	55 ± 1	62.5
26	100	74 ± 2	81.3
30	100	85 ± 2	93.8
20	66.7	87 ± 2	93.8
20	125	35 ± 1	50
30	150	55 ± 1	62.5
40	200	55 ± 1	62.5

The size of cloud and shell is also studied in nitrogen oxygen mixtures with lower and down to vanishing oxygen content. With decreasing oxygen concentration, the inception cloud becomes less pronounced until at the highest purity of nitrogen it seems not to exist at all. This different behaviour occurs because oxygen can store electrons by attachment and release them later again by detachment when the electric field exceeds the detachment threshold [16–18]. Nonlocal photo-ionization in nitrogen–oxygen mixtures further helps in making the discharge smoother.

4.1.2. Shell formation and stagnation. When the discharge develops further, the electrons drift in the high field towards tip and leave positive ions behind in the cloud. This charge separation decreases the electric field near the tip, and thus the ionization activity in this region decreases and stops eventually when the local field drops below the breakdown value. While the interior of the cloud gets electrically screened, the electric field in the outer region increases, actually to the value $E = U/R$ if the cloud of radius R is sufficiently conducting to transfer the complete tip voltage to its edge. If this electric field outside the cloud is above the breakdown value, the ionization reaction now continues in a shell-like region around the original cloud. In this manner the ionization transits from a bulk reaction in the cloud towards an ionization front in the shell that expands until the electric field on the surface reaches the breakdown value. The shell grows always slower than the initial cloud, it slows down towards the end of its evolution

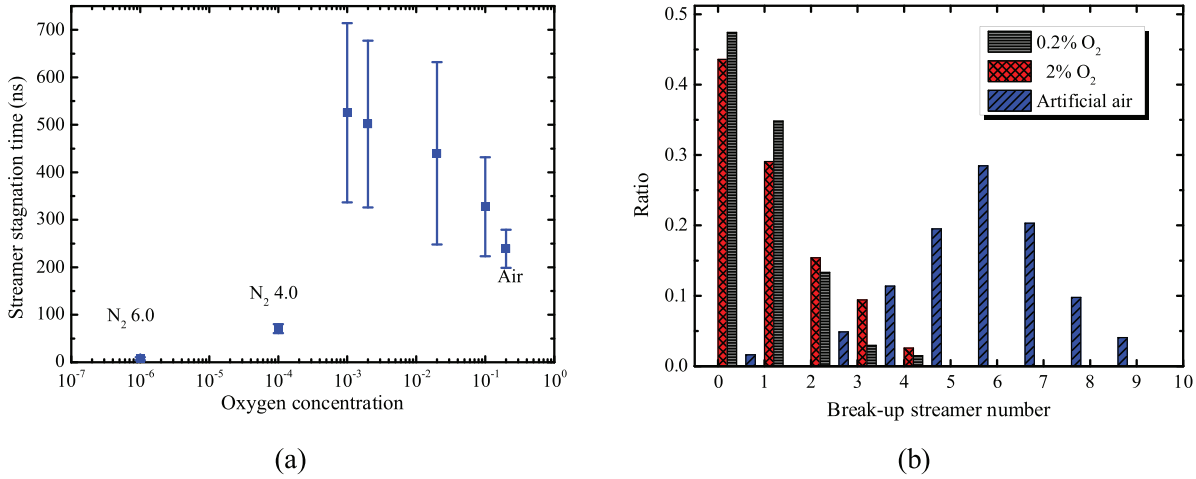

Figure 15. (*a*) Average streamer break-up time with error bar as a function of oxygen concentration. (*b*) Histogram of the number of break-up streamers for oxygen concentrations of 0.2, 2 and 20%. All data from measurements at 100 mbar and with 20 kV pulse amplitude at 1 Hz repetition frequency.

and transits into a stagnation phase. The stagnation indicates that the cloud has reached its maximal size, but that the symmetry breaking into streamers does not take place easily.

But in pure nitrogen, there is no shell formation, i.e. no space charge effects in the cloud. Rather the ionization avalanches directly form streamers, without cloud and shell formation and stagnation.

4.1.3. The velocities and their scaling with p. The initial growth of the cloud is the fastest stage of the discharge development. It is of the order of $10^6\,\mathrm{m\,s^{-1}}$. The fast initial growth is due to the high Laplacian field around the tip, which reaches $150\,\mathrm{kV\,cm^{-1}}$ at the tip for an applied voltage of 20 kV before the discharge starts (as calculated by Comsol Multiphysics). The oxygen ions can release free electrons in the small region where the field is larger than E_c; they initiate avalanches in the whole overvolted region, as recently simulated quantitatively with a 3D particle model in [16–18]. The growth at this stage probably occurs everywhere inside the region instantaneously. The shell phase, on the other hand, is probably similar to an ionization front.

Now for the same reduced electric field $|\mathbf{E}|/n$, or for the same U/p, the ionization front in the shell phase should have a velocity independent of n or p [37]. On the other hand, electron impact ionization and electron detachment from oxygen ions scale with the collision frequency which is proportional to p, i.e. the time scale of local avalanche growth scales like $1/p$. It is therefore surprising to see in figure 10, where p varies while U_p/p is fixed, that the scaling of cloud and shell phase seems to be just exchanged: the growth velocity of the initial cloud phase is independent of p (also when zooming into the figure), while the velocity in the shell phase scales roughly like $1/p$. This means that scaling with p works well for the size of the cloud, but not for its growth velocity. This observation will require future theoretical investigations. We finally remark that the different streamer velocities in figure 10 (appearing for discharge propagation distances larger than $R_{\max}$) are consistent with the fact that the streamer velocity increases with its reduced radius [45, 47].

4.2. The break-up of the cloud into streamers

4.2.1. Stagnation time and jitter. Figure 16(*a*) plots the streamer stagnation time as function of pressure in air for different voltage amplitudes. The streamer stagnation time is the time interval between the discharge inception and the break-up into streamers. The inception cloud is more stable at lower pressures. More specifically, the streamer stagnation time roughly scales with $1/p$ regardless of the voltage. The approximate relation between the stagnation time and the pressure is t = 240 ns bar/p, i.e. it scales with the collision frequency of electrons and ions with molecules. The jitter decreases with voltage and increases with pressure.

Figure 16(*b*) shows that the streamer stagnation time is almost the same for the three voltage amplitudes and the jitter decreases not much with the voltage. This confirms that the stagnation time is not influenced by the voltage amplitude though the inception cloud has a larger size for higher voltage. Furthermore, it can be inferred that the inception cloud develops at a higher velocity for higher voltage.

The influence of the repetition frequency is also shown in figure 16(*b*). The average stagnation time is quite similar for the three repetition rates. But the jitter of the stagnation time decreases with the repetition frequency. At lower repetition frequency less ionization is left behind from the previous discharge and the ionization level is estimated in [22]. Accordingly there are less free or attached electrons to initiate streamers at the edge of the inception cloud. At higher repetition frequency the background ionization level is enhanced which may facilitate the formation of streamers. This would explain the smaller jitter of streamer break-up time.

4.2.2. Number of streamers formed. A histogram of the number of streamers that emerge directly from the inception cloud at three repetition frequencies in 100 mbar air is shown in figure 11(*b*). The number of break-up streamers increases with repetition rate. But at 1 Hz and 10 Hz the distributions of streamer numbers are similar. If the ion diffusion is considered, the distribution of ionization is more homogeneous at lower repetition rate up to the point when the ion density is too low

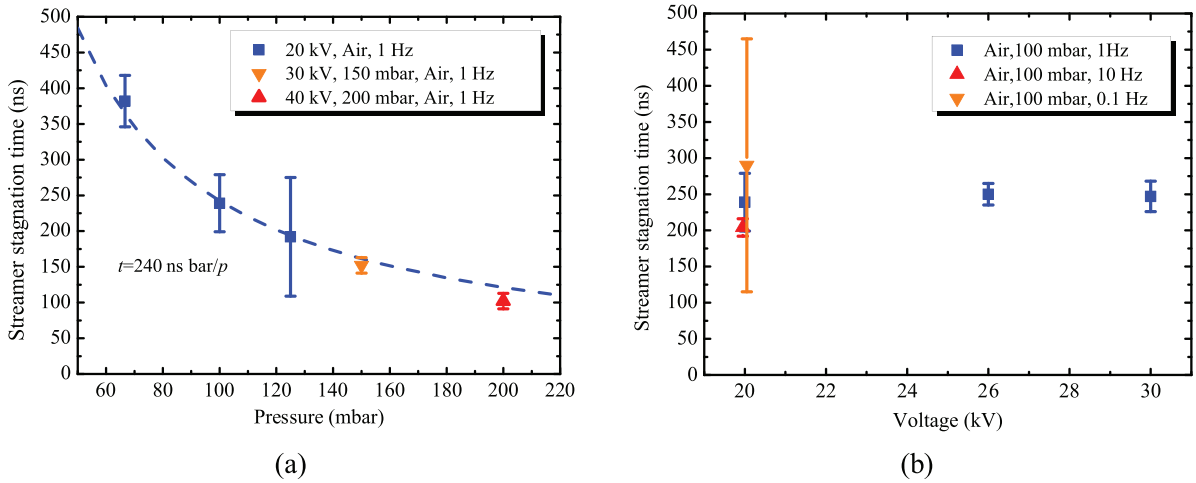

Figure 16. (*a*) Average stagnation time with standard deviation in air as function of pressure for different voltage amplitudes. (*b*) Average stagnation time with standard deviation in air as function of voltage for different pulse repetition frequencies.

[22]. It can be inferred that the inhomogeneous background ionization creates more streamers breaking up from the inception cloud. Figure 15(*b*) shows a histogram of the number of break-up streamers as function of oxygen concentration for concentrations of 0.2%, 2% and 20%. The number of break-up streamers reaches a minimum for 0.2% oxygen. These two results imply that the cloud is more stable at lower repetition rate or intermediate oxygen ratio, therefore it will break up in less streamers.

5. Conclusion

We have evaluated tens of thousands of pictures of the early stages of positive nanosecond pulsed discharges near a needle electrode in nitrogen–oxygen mixtures. There is a characteristic sequence of stages: first a rather spherical inception cloud is formed in the overvolted region (that some authors have called a diffuse discharge before). Then light is emitted from a shell around the previous cloud, which clearly indicates that the shell phase is driven by space charge effects. The radius of cloud and shell together is about 10% smaller than its theoretical maximum predicted by the ratio of applied voltage and breakdown field U_p/E_c. Then the discharge can stagnate after the shell phase until the symmetry is broken and streamers emerge; in some cases no streamers emerge at all.

There are characteristic differences between discharges in different nitrogen oxygen ratios. The size of the inception cloud decreases somewhat with decreasing oxygen ratio, and in the purest nitrogen no cloud seems to exist at all, rather streamers seem to emerge immediately near the electrode. Furthermore, the delay between discharge inception and streamer break-up also depends on oxygen concentration: the average stagnation time reaches its maximum value at approximately 0.1% oxygen, and the number of emerging streamers is the smallest; this indicates that the cloud is dynamically the most stable at this intermediate oxygen concentration. The streamer stagnation time roughly scales with $1/p$ regardless of the voltage, which indicates that it scales with the collision frequency of electrons and ions with molecules. An ionization front would have a velocity independent of p if the local reduced field $|\mathbf{E}|/p$ is the same. We remark that the length scales of the discharges agree well with predictions on scaling with pressure p, while the time scales raise questions, cf. section 4.1.3.

The different structures formed for different oxygen content can be roughly related to the following: first, oxygen can store electrons from previous discharges through attachment and release them when the local electric field exceeds the detachment value, and the oxygen ions are less mobile than free electrons; therefore electrons are more easily available at the next discharge pulse at higher oxygen content, and the memory of the previous discharge structure is more easily preserved. Second, the mixture of nitrogen and oxygen supports nonlocal photo-ionization which makes the discharges smoother. A more quantitative theoretical investigation of these observations is currently in preparation.

Acknowledgments

She Chen thanks D Trienekens, E van Veldhuizen and Ab Schrader in the EPG group at TU Eindhoven for useful suggestions on the experiments. His work in Eindhoven was supported by China Scholarship Council (201306210141), National Basic Research Program of China (Grant 2011CB209403) and Natural Science Foundation (51207078).

References

[1] van Veldhuizen E M and Rutgers W R 2002 Pulsed positive corona streamer propagation and branching *J. Phys. D: Appl. Phys.* **35** 2169–79
[2] Ono R and Oda T 2003 Formation and structure of primary and secondary streamers in positive pulsed corona discharge—effect of oxygen concentration and applied voltage *J. Phys. D: Appl. Phys.* **36** 1952–8
[3] Nudnova M M and Starikovskii A Y 2008 Development of streamer flash initiated by HV pulse with nanosecond rise time *IEEE Trans. Plasma Sci.* **36** 896–7
[4] Pai D Z, Stancu G D, Lacoste D A and Laux C O 2009 Nanosecond repetitively pulsed discharges in air at atmospheric pressure—the glow regime *Plasma Sources Sci. Technol.* **18** 45030

[5] Briels T M P, van Veldhuizen E M and Ebert U 2008 Time resolved measurements of streamer inception in air *IEEE Trans. Plasma Sci.* **36** 908–9

[6] Briels T M P, van Veldhuizen E M and Ebert U 2008 Positive streamers in air and nitrogen of varying density: experiments on similarity laws *J. Phys. D: Appl. Phys.* **41** 234008

[7] Ebert U *et al* 2011 Multiple scales in streamer discharges, with an emphasis on moving boundary approximations *Nonlinearity* **24** C1–26

[8] Liang X and Zhou Y 2003 *High Voltage Engineering* (Beijing: Tsinghua University)

[9] Sarma M P 2000 *Corona Performance of High Voltage Transmission Lines* (Hertfordshire: Research Studies)

[10] Goldman M and Sigmond R 1982 Corona and Insulation *IEEE Trans. Electr. Insul.* **EI-17** 90–105

[11] van Veldhuizen E M 2000 *Electrical Discharges for Environmental Purposes: Fundamentals and Applications* (New York: Nova Science Publishers)

[12] Winands G J J, Yan K, Pemen A J M, Nair S A, Liu Z and van Heesch E J M 2006 An industrial streamer corona plasma system for gas cleaning *IEEE Trans. Plasma Sci.* **34** 2426–33

[13] Masuda S 1988 Pulsed corona induced plasma chemical process: a horizon of new plasma chemical technologies *Pure Appl. Chem.* **60** 727–31

[14] Pancheshnyi S V, Lacoste D A, Bourdon A and Laux C O 2006 Ignition of propane-air mixtures by a repetitively pulsed nanosecond discharge *IEEE Trans. Plasma Sci.* **34** 2478–87

[15] Starikovskii A Y, Anikin N B, Kosarev I N, Mintoussov E I, Nudnova M M, Rakitin A E, Roupassov D V, Starikovskaia S M and Zhukov V P 2008 Nanosecond-pulsed discharges for plasma-assisted combustion and aerodynamics *J. Propul. Power* **24** 1182–97

[16] Sun A, Teunissen J and Ebert U 2013 Why isolated streamers do not exist in fields above breakdown in atmospheric air *Geophys. Res. Lett.* **40** 2417–22

[17] Teunissen J, Sun A and Ebert U 2014 A time scale for electrical screening in pulsed gas discharges *J. Phys. D: Appl. Phys.* **47** 365203

[18] Sun A, Teunissen J and Ebert U 2014 The inception of pulsed discharges in air: simulations in background fields above and below breakdown *J. Phys. D: Appl. Phys.* **47** 445205

[19] Nijdam S, Takahashi E, Teunissen J and Ebert U 2014 Streamer discharges can move perpendicularly to the electric field *New J. Phys.* **16** 103038

[20] Pancheshnyi S 2005 Role of electronegative gas admixtures in streamer start, propagation and branching phenomena *Plasma Sources Sci. Technol.* **14** 645–53

[21] Nijdam S, van de Wetering F M J H, Blanc R, van Veldhuizen E M and Ebert U 2010 Probing photo-ionization: experiments on positive streamers in pure gases and mixtures *J. Phys. D: Appl. Phys.* **43** 145204

[22] Nijdam S, Wormeester G, van Veldhuizen E M and Ebert U 2011 Probing background ionization: positive streamers with varying pulse repetition rate and with a radioactive admixture *J. Phys. D: Appl. Phys.* **44** 455201

[23] Abdel-Salam M and Allen N L 1990 Inception of corona and rate of rise of voltage in diverging electric fields *IEE Proc. A (Phys. Sci. Mea. Instrum. Manage. Educ.)* **137** 217–20

[24] Lowke J J and D'Alessandro F 2003 Onset corona fields and electrical breakdown criteria *J. Phys. D: Appl. Phys.* **36** 2673

[25] van Veldhuizen E M and Rutgers W R 2003 Inception behaviour of pulsed positive corona in several gases *J. Phys. D: Appl. Phys.* **36** 2692–6

[26] Mcallister I W, Crichton G C and Bregnsbo E 1979 Experimental study on the onset of positive corona in atmospheric air *J. Appl. Phys.* **50** 6797–805

[27] Naidis G V 2005 Conditions for inception of positive corona discharges in air *J. Phys. D: Appl. Phys.* **38** 2211

[28] Ortéga P, Heilbronner F, Rühling F, Díaz R and Rodière M 2005 Charge–voltage relationship of the first impulse corona in long airgaps *J. Phys. D: Appl. Phys.* **38** 2215–26

[29] Tardiveau P, Moreau N, Bentaleb S, Postel C and Pasquiers S 2009 Diffuse mode and diffuse-to-filamentary transition in a high pressure nanosecond scale corona discharge under high voltage *J. Phys. D: Appl. Phys.* **42** 175202

[30] Pechereau F, Le Delliou P, Jansky J, Tardiveau P, Pasquiers S and Bourdon A 2014 Large conical discharge structure of an air discharge at atmospheric pressure in a point-to-plane geometry *IEEE Trans. Plasma Sci.* **42** 2346–7

[31] Nijdam S, Miermans K, van Veldhuizen E M and Ebert U 2011 A Peculiar streamer morphology created by a complex voltage pulse *IEEE Trans. Plasma Sci.* **39** 2216–7

[32] Luque A, Ratushna V and Ebert U 2008 Positive and negative streamers in ambient air: modeling evolution and velocities *J. Phys. D: Appl. Phys.* **41** 234005

[33] Clevis T T J, Nijdam S and Ebert U 2013 Inception and propagation of positive streamers in high-purity nitrogen: effects of the voltage rise rate *J. Phys. D: Appl. Phys.* **46** 45202

[34] Pasko V P 2007 Red sprite discharges in the atmosphere at high altitude: the molecular physics and the similarity with laboratory discharges *Plasma Sources Sci. Technol.* **16** S13

[35] Ebert U, Nijdam S, Li C, Luque A, Briels T M P and van Veldhuizen E 2010 Review of recent results on streamer discharges and discussion of their relevance for sprites and lightning *J. Geophys. Res. Space Phys.* **115** A00E43

[36] Liu N and Pasko V P 2006 Effects of photoionization on similarity properties of streamers at various pressures in air *J. Phys. D: Appl. Phys.* **39** 327–34

[37] Ebert U, Montijn C, Briels T M P, Hundsdorfer W, Meulenbroek B, Rocco A and van Veldhuizen E M 2006 The multiscale nature of streamers *Plasma Sources Sci. Technol.* **15** S118–29

[38] Pasko V P, Inan U S and Bell T F 1998 Spatial structure of sprites *Geophys. Res. Lett.* **25** 2123–6

[39] Gordillo-Vázquez F J and Luque A 2010 Electrical conductivity in sprite streamer channels *Geophys. Res. Lett.* **37** L16809

[40] Luque A and Gordillo-Vázquez F J 2011 Mesospheric electric breakdown and delayed sprite ignition caused by electron detachment *Nat. Geosci.* **5** 22–5

[41] Liu N 2012 Multiple ion species fluid modeling of sprite halos and the role of electron detachment of O^- in their dynamics *J. Geophys. Res.: Space Phys.* **117** A3308

[42] Kos J, Briels T M P, van Veldhuizen E M and Ebert U 2006 Circuit dependence of the diameter of pulsed positive streamers in air *J. Phys. D: Appl. Phys.* **39** 5201–10

[43] Nijdam S, Geurts C G C, van Veldhuizen E M and Ebert U 2009 Reconnection and merging of positive streamers in air *J. Phys. D Appl. Phys.* **42** 045201

[44] Nudnova M M and Starikovskii A Y 2008 Streamer head structure: role of ionization and photoionization *J. Phys. D: Appl. Phys.* **41** 234003

[45] Briels T M P, Kos J, Winands G J J, Van Veldhuizen E M and Ebert U 2008 Positive and negative streamers in ambient air: measuring diameter, velocity and dissipated energy *J. Phys. D: Appl. Phys.* **41** 234004

[46] Luque A, Ebert U, Montijn C and Hundsdorfer W 2007 Photoionization in negative streamers: fast computations and two propagation modes *Appl. Phys. Lett.* **90** 081501

[47] Naidis G V 2009 Positive and negative streamers in air: velocity-diameter relation *Phys. Rev.* E **79** 57401